


Negative Impact of Aromatase Inhibitors on Proximal Femoral Bone Mass and Geometry in Postmenopausal Women with Breast Cancer

Su Jin Lee¹ · Kyoung Min Kim² · J. Keenan Brown³ · Alan Brett³ · Yun Ho Roh⁴ · Dae Ryong Kang⁴ · Byeong Woo Park⁵ · Yumie Rhee^{1,6} 

Received: 14 March 2015 / Accepted: 24 July 2015 / Published online: 1 August 2015
© Springer Science+Business Media New York 2015

Abstract Aromatase inhibitors (AIs), the standard therapy for estrogen receptor- or progesterone receptor-positive breast cancer in postmenopausal women, lead to increased hip fractures in breast cancer patients. To investigate the mechanism of increased incidence of hip fractures in breast cancer patients treated with AIs, we evaluated bone mineral density (BMD) in the cortical and trabecular compartments and assessed femoral geometry using quantitative computed tomography (QCT) in breast cancer patients. In total, 249 early breast cancer patients who underwent QCT in their fifties (mean age 54.3 years) were retrospectively analyzed. Proximal femoral BMD and geometrical parameters were compared. In all regions of the proximal femur, cortical areal BMDs were lower in the AI group than in the non-AI group ($p < 0.05$). Cortical thickness of the femoral neck, trochanter, and total hip was significantly lower in the AI group compared with the non-

AI group ($p < 0.05$). Analysis of the narrowest section of the femoral neck showed significantly thinner cortical bone and smaller cortical area in the AI group than in the non-AI group ($p < 0.05$), especially in the superoposterior quadrant. Bone strength parameters in the femoral neck, such as the section modulus and cross-sectional moment of inertia, were significantly lower in the AI group than in the non-AI group ($p < 0.05$). In conclusion, AI treatment in breast cancer patients is associated with deterioration of femoral cortical BMD and geometry, which could contribute in site-specific weakened bone strength and increased incidence of hip fractures.

Keywords Aromatase inhibitor · Breast cancer · Quantitative computed tomography · Bone geometry · Bone strength

Introduction

Breast cancer is associated with exposure to increased levels of estrogen [1, 2]. Accordingly, postmenopausal women with hormone-responsive breast cancer (estrogen receptor- or progesterone receptor-positive) are treated with aromatase inhibitors (AIs) to reduce estrogen levels and prevent recurrence after mastectomy [3–6]. However, AIs accelerate bone loss and increase the risk of osteoporotic fractures due to total ablation of peripheral estrogen production [7, 8]. Previous studies showed that postmenopausal survivors of breast cancer are at increased fracture risk and women taking AIs were found to have an increased risk of vertebral fracture [1, 9, 10]. Vertebrae are primarily composed of trabecular bone, which is metabolically active and rapidly affected by estrogen deficiency; therefore, the risk of vertebral fractures

✉ Yumie Rhee
yumie@yuhs.ac

¹ Department of Internal Medicine, Severance Hospital, Endocrine Research Institute, Yonsei University College of Medicine, 50-1 Yonsei-ro, Seodaemun-gu, Seoul 120-752, Korea
² Department of Internal Medicine, Seoul National University Bundang Hospital, Seongnam, Korea
³ Mindways Software Inc., Austin, TX, USA
⁴ Biostatistics Collaboration Unit, Yonsei University College of Medicine, Seoul, Korea
⁵ Division of Breast Surgery, Department of Surgery, Severance Hospital, Yonsei University College of Medicine, Seoul, Korea
⁶ Avison Biomedical Research Center, Yonsei University College of Medicine, Seoul, Korea

increases in breast cancer patients treated with AIs. However, the United States Food and Drug Administration Adverse Event Reporting System database revealed that from January 1998 to December 2008, the incidence of hip or femoral fracture among women aged <65 years undergoing breast cancer therapy (226 fracture cases) was 19 %, which is higher than the incidence of vertebral fractures [11]. In that study, AIs were the most common drugs associated with fractures. Furthermore, hip fractures occurred much earlier in women with breast cancer than in healthy women [11–16].

Many studies have reported the negative effect of AIs on bone mineral density (BMD) using dual-energy X-ray absorptiometry (DXA) [8, 16–20]. However, BMD alone cannot fully explain why fractures occur more especially at hip where cortical component is more dominant than trabecular component. DXA measures integral (cortical and trabecular) areal BMD (aBMD). While hip structure analysis (HSA) method that reports measures such as average cortical thickness have been applied to DXA hip images, this method depends sensitively upon assumptions regarding bone shape and the average partitioning of bone mineral between cortical and trabecular compartments. Deviations from these assumptions bias HSA measurements and complicate their interpretation. Thus, we used quantitative computed tomography (QCT) in this study to further evaluate the femoral geometry [21–25]. At the hip, QCT-assessed changes in bone geometry, such as cortical thickness and buckling ratio (BR), which affect bone strength, may be helpful parameters to understand the mechanism underlying hip fractures [26]. Furthermore, QCT of the spine can be used to measure BMD only within the vertebral trabecular bone. Vertebral trabecular bone is important for the structural integrity of the spine, and limiting this measurement to trabecular bone eliminates confounding factors associated with factors such as inclusion of spinous processes, osteophytes, and joint spacing that affect BMD measurements by DXA.

We hypothesized that the changes by AIs in the geometric parameters besides the BMD of proximal femur would contribute to increased hip fractures occurring in postmenopausal women with breast cancer patients treated with AIs.

Materials and Methods

Study Subjects

Breast cancer patients who visited Severance Hospital between June 2009 and January 2012 were reviewed retrospectively. Among the patients after mastectomy, a total of 436 subjects who also had undergone bone evaluation by

QCT were collected (Fig. 1). Patients who were premenopausal or over 60 years old and patients with any metastatic breast cancer ($n = 4$), other malignancies ($n = 13$), renal failure ($n = 2$), and on any medications that can affect bone metabolism, such as glucocorticoids ($n = 12$), bisphosphonates ($n = 10$), selective estrogen receptor modulators (SERM) ($n = 2$) were excluded. Finally, 249 postmenopausal women aged 50–59 years with early-stage breast cancer (stage 1 or 2) were analyzed. According to hormone receptor status, estrogen receptor- and progesterone receptor-negative breast cancer patients, who did not require AI treatment after mastectomy, were assigned to non-AI group, and estrogen receptor- or progesterone receptor-positive breast cancers patients who started additional adjuvant AI treatment were assigned to AI group. The length of treatment with AI was calculated by the days from the time of starting AI treatment to the time of QCT scan for subjects. The study was approved by the Institutional Review Board of Yonsei University Health System (IRB, No.4-2013-0685).

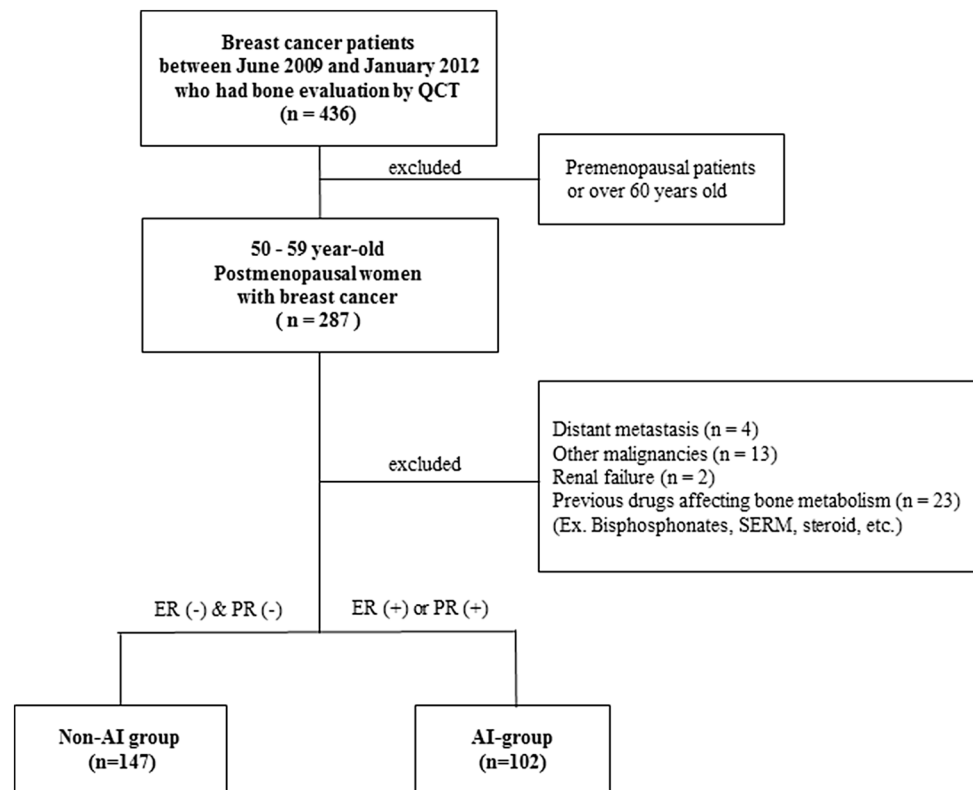
Biochemical and Hormonal Assays

Routine biochemical parameters, including the levels of calcium, inorganic phosphate, albumin, blood urea nitrogen, and creatinine were measured. Blood samples were collected in the morning after an overnight fast. Bone turnover markers, such as carboxy-terminal cross-linking telopeptide of type 1 collagen (CTX) (Osteomark; Ostex International, Seattle, WA, USA) and osteocalcin (CIS Bio International, Gif-sur-Yvette, France), were measured by enzyme-linked immunosorbent assay. The intra- and interassay coefficients of variation (%) were <5.8 and <5.9 % for CTX and <2.0 and <5.0 % for osteocalcin, respectively.

QCT Scanning

Subjects were scanned on a GE LightSpeed VCT (GE Medical Systems, Milwaukee, WI, USA) at 120 kVp, 120 mAs using a 50-cm scan field-of-view. CT images were reconstructed with a standard body reconstruction algorithm at 2.5-mm intervals with a 2.5-mm slice thickness. A 36-cm display field-of-view was used resulting in an in-plane pixel size of approximately 0.7 mm. Lumbar BMD (mg/cm^3 , K_2PHO_4) was calculated as the average volumetric BMD (vBMD) of L1 and L2. Each lumbar vBMD was measured in an automatically placed elliptical trabecular region of interest with 9-mm cylinder height, positioned at midlevel. All scanned data were analyzed by QCT PRO software (Mindways Software, Austin, TX, USA) and the CTXA Hip Exam Analysis protocol (Mindways Software, Austin, TX, USA). Series of equally

Fig. 1 Flowchart of study subjects. A total of 249 postmenopausal women aged 50–59 years with breast cancer examined by QCT were analyzed. Abbreviations: *QCT* quantitative computed tomography, *ER* estrogen receptor, *PR* progesterone receptor, *AI* aromatase inhibitor



spaced axial images through proximal femur were scanned, then soft-tissue pixels from axial images were removed. By summation of mineral mass and bone volume along the path of the X-ray beam, the projection image of the femur shown in the same direction as that in the DXA projection was synthesized (Fig. 2a). The proximal femur was divided into the femoral neck, trochanter, and intertrochanter. The

total hip included all of the femoral neck, trochanter, and intertrochanter. Each bone pixel identified by QCT was further classified as being most representative of either “cortical” or “trabecular” bone, with a cortical threshold of 350 mg/cm^3 . Average cortical bone depth along the projection direction used to measure area density was calculated as a surrogate for cortical thickness. Average

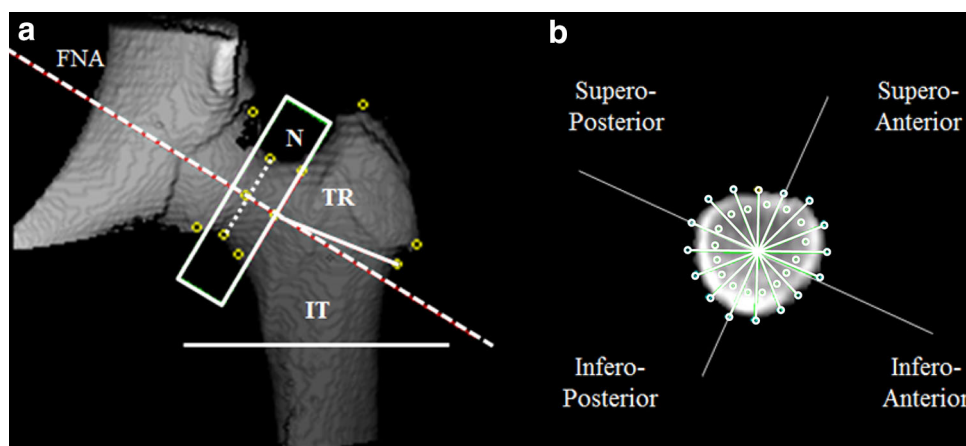


Fig. 2 Region of interest of the proximal femur defined by quantitative computed tomography. **a** Each part (N, TR, and IT) is demarcated by a *solid line*. The height of the N box is 15 mm. The FNA is defined by a *long dotted line* across the narrowest portion of the N and orthogonal to the *short dotted line*, passing through the

midpoint of the *short dotted line*. **b** The narrowest cross -section of the N is classified into 4 quadrants: superoposterior, superoanterior, inferoposterior, and inferoanterior. Abbreviations: *N* femoral neck, *TR* trochanter, *IT* intertrochanter, *FNA* femoral neck axis

cortical depth of ROI is given by the ratio of the ROI volume to ROI projected area. BR, defined as the ratio of the radius over cortical thickness, was also calculated [24, 26, 27].

Regional Geometry and Bone Strength Parameters of the Femur

To further analyze regional geometry and bone strength parameters in the narrowest cross section of the femoral neck, we used the QCT PRO Bone Investigational Toolkit (BIT) software (Mindways Software, Austin, TX, USA). The analysis method used for this study is similar to that used by Poole et al. except that the femoral neck was characterized in our current study at the narrowest part of the neck [35]. Briefly, the narrowest cross section of the femoral neck was selected and divided into 16 sectors defined by equal arc length. Thereafter, all sectors were reclassified into 4 quadrants: superoposterior, superoanterior, inferoposterior, and inferoanterior (Fig. 2b). Cortical and trabecular vBMD, cross-sectional area, and average cortical thickness in the 4 quadrants were analyzed. Bone strength parameters, such as section modulus (Z) and cross-sectional moment of inertia (CSMI), were also measured.

Statistical Analysis

Differences in clinical characteristics and bone parameters between the AI and non-AI groups were compared using the Student's t test. Data were represented as the mean \pm standard deviation. p values <0.05 were considered statistically significant. Bone strength parameters, Z and CSMI, were compared by analysis of covariance (ANCOVA) with adjustment for age and body mass index (BMI). Multiple linear regressions were performed to determine the independent association between the AI treatment and dependent variables such as cortical aBMD and cortical thickness of neck, trochanter, intertrochanter, and total hip. In this model, age and BMI were included as covariates. All statistical analyses were performed using SPSS version 20.0 (IBM Corporation, Armonk, NY, USA).

Results

Subject Characteristics

Table 1 presents the clinical characteristics of the study subjects. The averages of age at the time of QCT scan were 54.1 ± 2.7 years in the non-AI group and 54.7 ± 2.5 years in the AI group, respectively. There were no significant differences between the 2 groups with respect to age and

Table 1 Clinical characteristics of study subjects

	Non-AI group $n = 147$	AI group $n = 102$
Age (yr)	54.1 ± 2.7	54.7 ± 2.5
BMI (kg/m^2)	23.4 ± 2.8	23.7 ± 2.9
AIs (%)		
Anastrozole	–	54.9
Letrozole	–	45.1
The mean length of treatment time with AI, mo	–	24.0 ± 14.4
Previous radiotherapy [n (%)]	109 (74.1 %)	69 (67.6 %)
Biochemical parameters		
Calcium (mg/dL)	9.3 ± 0.3	9.4 ± 0.3
Phosphorus (mg/dL)	3.8 ± 0.4	3.9 ± 0.3
Albumin (g/dL)	4.5 ± 0.6	4.5 ± 0.5
BUN (mg/dL)	13.6 ± 3.2	13.5 ± 2.7
Creatinine (mg/dL)	0.7 ± 0.1	0.7 ± 0.1

Values represent the mean \pm standard deviation

yr years, AI aromatase inhibitor, BMI body mass index, mo months, BUN blood urea nitrogen

BMI. In the AI group, 2 different types of AIs were used—anastrozole (54.9 %) and letrozole (45.1 %)—and the mean length of treatment with AI at the time of the CT scan was 24.0 ± 14.4 months. The percent of the subjects who had previous radiotherapy were 74.1 % in non-AI group and 67.6 % in AI-group. Biochemical parameters including calcium, phosphorus, albumin, blood urea nitrogen, and creatinine showed no significant difference between two groups.

Bone Turnover Markers and BMD of the Spine and Femur

The mean CTx level of the AI group was 41.2 % higher than that of the non-AI group ($p = 0.001$) (Table 2). However, the mean osteocalcin levels of the 2 groups were not significantly different. The average vBMD of the lumbar spine in the AI group was 2.8 % lower than that in the non-AI group, but this difference was not significant. The AI group did show significantly lower integral and cortical aBMD of the total hip compared with the non-AI group (4.1 vs. 6.4 %; $p < 0.05$). When analyzing each part of the femur (neck, trochanter, and intertrochanter) (Table 2), all measurements of aBMD in the integral and cortical compartments in the AI group were lower than those in the non-AI group (all, $p < 0.05$). However, trabecular aBMD was significantly lower in the AI group compared with the non-AI group only in the trochanter region (lower by 2.7 %; $p < 0.05$).

Changes in Bone Strength Parameters and Regional Geometry of the Femur

Compared to the non-AI group, average cortical depth in the AI group was significantly lower in the femoral neck by 10.0 % ($p = 0.007$), trochanter by 11.4 % ($p = 0.036$), intertrochanter by 2.5 % ($p = 0.241$), and total hip by 5.1 % ($p = 0.014$). The AI group had a relatively higher BR compared with the non-AI group, but this difference was not significant. According to analysis by QCT PROBIT to measure regional differences of narrow neck around four quadrants, the average cortical area and cortical thickness were lower in the AI group compared with the non-AI group; however, only the superoposterior quadrant had thinner cortical area and cortical thickness, which was reduced by 20.0 and 20.6 % ($p = 0.004$ and 0.011, respectively) in the AI group compared to non-AI group, respectively (Table 3). AI group also showed significantly decreased bone strength parameters of Z and CSMI after adjustment for age and BMI (all, $p < 0.05$) (Fig. 3).

Association of AI Treatment with BMD and Bone Geometry

Association of AI treatment on cortical aBMD and cortical thickness in each part of the proximal femur (neck, trochanter, intertrochanter, and total hip) was further analyzed by regression analysis for the adjustment for age and BMI. AI treatment had significantly lower cortical aBMD [$\beta = -0.026$, standard error (SE) = 0.013, $p = 0.039$ at the neck; $\beta = -0.03$, SE = 0.014, $p = 0.03$ at the intertrochanter; $\beta = -0.028$, SE = 0.012, $p = 0.015$ at the total hip) (Table 4a). Cortical thickness of the femoral neck and total hip ($\beta = -0.047$, SE = 0.018, $p = 0.011$; $\beta = -0.036$, SE = 0.015, $p = 0.021$, respectively) were also negatively affected by AI use (Table 4b). In addition, BR showed the trend to be higher in the AI group compared to the non-AI group (Data not shown).

Discussion

This study demonstrated that AI treatment in early postmenopausal women with hormone-responsive breast cancer is associated with the deterioration of proximal hip BMD and geometry, leading to weakened bone strength. Compared with the non-AI group, the integral and cortical aBMD of all regions of the proximal hip, along with the cortical thickness of the femoral neck, trochanter, and total hip were lower in the AI group; moreover, bone strength parameters were lower in the AI group compared to the non-AI group. In addition, both the average cortical area and thickness of the superoposterior quadrant of the

Table 2 Bone parameters of study subjects

	Non-AI group <i>n</i> = 147	AI group <i>n</i> = 102
Serum bone turnover marker		
CTx (ng/mL)*	0.51 ± 0.5	0.72 ± 0.5 ^a
Osteocalcin (ng/mL) ^c	22.2 ± 14.7	25.0 ± 10.3
Density parameters of the spine and femur		
Lumbar spine—volumetric BMD (mg/cc)	109.3 ± 29.7	106.2 ± 24.1
Femur—aBMD (g/cm ²)		
Integral compartment		
Neck	0.669 ± 0.107	0.636 ± 0.091 ^b
Trochanter	0.590 ± 0.093	0.562 ± 0.088 ^b
Intertrochanter	0.974 ± 0.130	0.934 ± 0.120 ^b
Total	0.790 ± 0.107	0.758 ± 0.105 ^b
Trabecular compartment		
Neck	0.248 ± 0.044	0.247 ± 0.049
Trochanter	0.329 ± 0.032	0.320 ± 0.032 ^b
Intertrochanter	0.278 ± 0.036	0.272 ± 0.039
Total	0.289 ± 0.028	0.283 ± 0.300
Cortical compartment		
Neck	0.420 ± 0.102	0.392 ± 0.090 ^b
Trochanter	0.262 ± 0.082	0.242 ± 0.071 ^b
Intertrochanter	0.696 ± 0.118	0.662 ± 0.102 ^b
Total	0.501 ± 0.095	0.469 ± 0.086 ^b
Geometric parameters of the proximal femur		
Average cortical depth (cm)		
Neck	0.50 ± 0.15	0.45 ± 0.13 ^b
Trochanter	0.35 ± 0.14	0.31 ± 0.13 ^b
Intertrochanter	0.80 ± 0.14	0.78 ± 0.20
Total	0.59 ± 0.13	0.56 ± 0.11 ^b
Buckling ratio		
Neck	5.06 ± 1.93	5.55 ± 2.90
Trochanter	10.84 ± 9.31	11.92 ± 9.06
Intertrochanter	3.71 ± 0.82	3.84 ± 0.77
Total	4.91 ± 1.17	5.13 ± 1.24

Values represent the mean ± standard deviation

* Non-AI versus AI ($n = 142$ vs. $n = 101$)

^a $p < 0.001$

^b $p < 0.05$ (vs. non-AI group by Student's *t* test)

^c non-AI vs. AI ($n = 139$ vs. $n = 101$)

narrowest cross-section of the femoral neck were the lowest among 4 quadrants, and these were significantly lower in the AI group than in the non-AI group, thus showing a regional difference.

AIs are the treatment of choice for postmenopausal women with hormone-responsive breast cancer as they prevent recurrence by decreasing remnant estrogen levels [28]. As estrogen suppresses the rate of bone remodeling and controls the apoptotic balance among osteocytes,

Table 3 Regional differences in bone geometric parameters of the femoral neck

	Non-AI group <i>n</i> = 57	AI group <i>n</i> = 61
Superoposterior		
Cortical vBMD (mg/cm ³)	385.42 ± 52.67	367.01 ± 60.33
Trabecular vBMD (mg/cm ³)	79.33 ± 21.96	81.08 ± 18.61
Cortical area (cm ²)	0.42 ± 0.17	0.34 ± 0.14 ^a
Cortical thickness (mm)	2.04 ± 1.04	1.62 ± 0.72 ^a
Superoanterior		
Cortical vBMD (mg/cm ³)	408.64 ± 40.54	397.67 ± 45.14
Trabecular vBMD (mg/cm ³)	74.45 ± 24.40	77.53 ± 16.50
Cortical area (cm ²)	0.55 ± 0.17	0.50 ± 0.17
Cortical thickness (mm)	2.46 ± 0.90	2.27 ± 0.82
Inferoposterior		
Cortical vBMD (mg/cm ³)	575.51 ± 63.46	582.20 ± 55.11
Trabecular vBMD (mg/cm ³)	35.62 ± 34.18	38.30 ± 34.45
Cortical area (cm ²)	0.90 ± 0.16	0.86 ± 0.14
Cortical thickness (mm)	4.83 ± 0.94	4.60 ± 0.78
Inferoanterior		
Cortical vBMD (mg/cm ³)	541.67 ± 72.60	531.67 ± 57.82
Trabecular vBMD (mg/cm ³)	15.80 ± 33.15	21.69 ± 27.50
Cortical area (cm ²)	0.89 ± 0.14	0.84 ± 0.15
Cortical thickness (mm)	5.06 ± 0.97	4.73 ± 0.90

AI aromatase inhibitor, vBMD volumetric bone mineral density

Values represent the mean ± standard deviation

^a *p* < 0.05 (vs. non-AI group by Student's *t* test)

osteoblasts, and osteoclasts, estrogen deprivation therapy can increase bone remodeling [29]. The levels of bone resorption markers were significantly higher in the AI

group, which could reflect negative bone balance caused by further estrogen deprivation by additional AI treatment (Table 2). With regard to BMD, the average vBMD of the lumbar spine, composed mainly of trabecular bone, was not significantly different between the AI and non-AI group. This may be explained by rapid trabecular bone loss already occurred following menopause and previous adjuvant chemotherapies in both groups. On the other hand, the average cortical BMD of the proximal hip, which is composed of an equal amount or more of cortical bone, was significantly lower in the AI group. Since estrogen can not only attenuate cancellous resorption but also vitiate cortical bone loss, AI administration could lead to cortical deterioration in addition to the loss of trabecular bone [30, 31].

AI-associated bone loss increases the risk of osteoporotic fractures [16, 17, 19, 32]. In the general population, hip fractures increase in the eighth decade of life [15]. However, a recent study showed that hip fractures can occur at a younger age, particularly in breast cancer patients aged <50 years, with a hazard ratio of 5.32 (95 % confidence interval, 2.30–12.3), and in breast cancer patients aged between 50 and 64 years, with a hazard ratio of 2.30 (95 % confidence interval, 1.43–3.67) [16]. To explain the earlier femoral failure load in breast cancer patients, QCT measurement of cortical and trabecular BMD, as well as geometric variables, could be helpful [33]. Since increased endocortical resorption with subsequent cortical thinning is a potential factor leading to hip fracture [34], we estimated the cortical thickness and BR using QCT. BR is related to cortical instability and reflects the ability of bone to resist bending forces at the tensile surface. Increasing BR is associated with the increasing risk of fracture. Consistent with this concept, our results

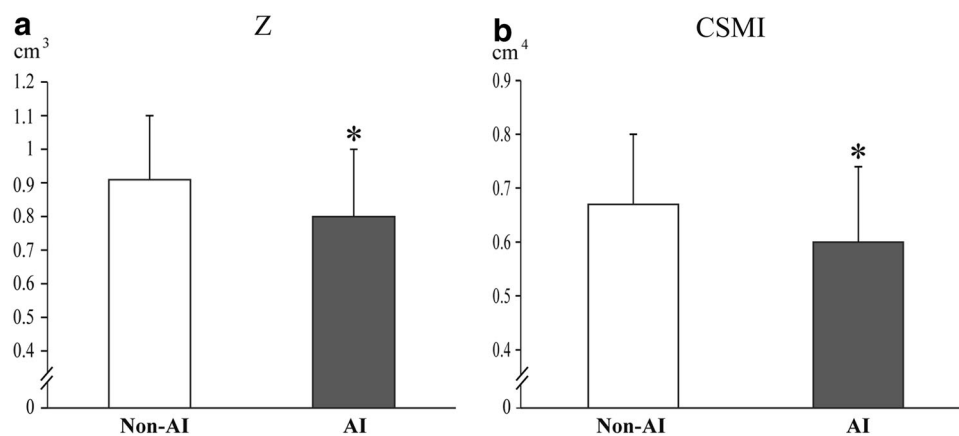


Fig. 3 Bone strength parameters in the AI group were significantly lower than those in the non-AI group. Z and CSMI of the narrowest cross section of the proximal femoral neck were significantly lower in the AI group compared with the non-AI group. The white box indicates the non-AI group, and the black box indicates the AI group.

Boxes and error bars represent the mean and standard deviation, respectively. Abbreviations: AI aromatase inhibitor, Z section modulus, CSMI cross-sectional moment of inertia. **p* < 0.05 according to ANCOVA adjusted by age and BMI

Table 4 Effects of AI on cortical aBMD and thickness

Variables	Neck			Trochanter			Intertrochanter			Total hip		
	β	SE	<i>p</i> value	β	SE	<i>p</i> value	β	SE	<i>p</i> value	β	SE	<i>p</i> value
a. Cortical aBMD												
Age	-0.005	0.002	0.035	-0.006	0.002	0.001	-0.01	0.003	0.001	-0.008	0.002	0.001
BMI	0.003	0.002	0.227	0.005	0.002	0.002	0.008	0.002	0.001	0.005	0.002	0.013
AI treatment	-0.026	0.013	0.039	-0.008	0.01	0.061	-0.03	0.014	0.03	-0.028	0.012	0.015
b. Cortical thickness												
Age	-0.007	0.003	0.045	-0.012	0.003	0.001	-0.016	0.004	0.001	-0.011	0.003	0.001
BMI	0.004	0.003	0.235	0.008	0.003	0.004	0.009	0.004	0.013	0.009	0.003	0.002
AI treatment	-0.047	0.018	0.011	-0.032	0.017	0.055	-0.019	0.021	0.364	-0.036	0.015	0.021

Bold means the *p* value under 0.05

The basic model was adjusted for age and BMI

Cortical aBMD and cortical thickness of the 4 parts were analyzed as dependent variables. Coefficients (β) are shown with standard error (SE) analyzed by multiple linear regressions

AI aromatase inhibitor, aBMD areal bone mineral density, SE standard error, BMI body mass index

demonstrated a lower cortical thickness in the neck, trochanter, and total hip, and a relatively high BR, in the AI group compared with the non-AI group (Table 2).

The regional difference of cortical thickness in the narrow-neck section is important to compensate for mechanical loading during aging [14, 35]. Adaptive remodeling for tensile stresses at the superior region of the femoral neck and compressive stresses at the inferior region results in differential cortical thinning, with relative preservation of the inferior region [36]. Our results also found a similar pattern of asymmetry in the femoral neck cross section, with the cortical area and thickness being lowest in the superoposterior quadrant and the highest in the inferoposterior quadrant (Table 3). Furthermore, when we compared the two groups, cortical area and thickness in the superoposterior quadrant in AI group were significantly lower in the AI group compared with the non-AI group. As the superoposterior quadrant is already thin and vulnerable to fracture, accelerated cortical thinning related with AI treatment in this area could contribute to the higher occurrence of femoral neck fractures at an earlier age in breast cancer patients. Of course, these findings could reflect a partial volume error because the thickness of cortical bone is very thin in the superior regions of the femoral neck approaching 1 mm or less [37]. Cortical BMD is a measurement that is sensitive to factors other than changes in true cortical BMD. Inferior structure could include dense trabecular bone that may have a BMD above 350 mg/cc, which is classified as “cortical” bone by the BIT analysis resulting in an upward bias in cortical thickness and cortical CSA estimates, in content with a corresponding downward bias in trabecular bone [38].

As deteriorated cortical bone could be affected by aging and BMI, we also adjusted for these variables to assess the

effect of AI treatment on cortical aBMD and thickness. AI treatment independently and negatively affected cortical aBMD at the femoral neck, intertrochanter, and total hip. Deteriorated cortical bone at the femoral neck and total hip induced by AI treatment was independently related. Age and BMI—adjusted means of Z and CSMI, which reflect the ability of bone to resist bending forces at the compressive surface of the cortical compartment, were significantly lower in the AI group compared with the non-AI group (Fig. 3). Decreases in strength parameters in the narrowest cross section of the femoral neck could provide another plausible explanation of why hip fractures may occur as early as the sixth decade of life in postmenopausal women with breast cancer treated with AIs.

Our study had certain limitations. First, this was a cross-sectional study of 249 postmenopausal women with breast cancer. Baseline QCT data before starting AI in the AI-group were not collected, thus causal effects of AI on bone were not measured. However, additional AI treatment could negatively affect bone strength of hormone receptor-positive breast cancer patients compared to that of hormone receptor-negative breast cancer who are not treated with AI. Further studies are needed to compare longitudinal changes in bone parameters within and between groups, by collecting serial data of the study subjects to confirm the extent to which the AI treatment negatively affects BMD and bone strength. Second, we were unable to analyze the incidence of hip fracture as an outcome in this study. To confirm our hypothesis, a further long-term prospective study should be performed. Third, even though physical activity is an important factor in determining both size and geometry of the bone, our study did not evaluate patients in this aspect. However, Eastern Cooperative Oncology Group (ECOG) status of those patients was fully active (grade 0) or

ambulatory and able to carry out light house or office work (grade 1) [39]. Last, the resolution of our QCT data was not sufficient to analyze intracortical remodeling and cortical porosity or to avoid the partial volume effect [40].

Nevertheless, our study also has strengths. There has been a paucity of data on the relationship between geometric parameters of the proximal hip and increased risk of hip fracture in breast cancer patients treated with AIs. The previous studies reported the negative impact of AIs on vBMD and cortical thickness by high-resolution peripheral QCT analyzing only *peripheral* extremities as the regions of interest [41, 42]. Instead, we directly analyzed the *proximal hip* geometric characteristics to determine the hip structural alteration caused by AIs with QCT [43]. We examined not only the BMD but also the bone geometric parameters of every part of the proximal femur, as well as bone strength parameters and regional differences among the 4 quadrants of the narrowest cross section of the femoral neck [26]. To our knowledge, this is the first study to use QCT to analyze proximal hip geometric characteristics of patients treated with AIs in postmenopausal women in breast cancer.

In conclusion, AI treatment is negatively associated with deterioration of not only BMD but also the geometry of the proximal femur. Reduced BMD and bone strength of cortical compartment with regional differences in the narrowest cross section of the femoral neck in AI group may provide plausible mechanisms for the increased incidence of hip fracture in this patient population. Additional prospective research on femoral geometry is necessary to predict the fracture risk and to establish proper management of AI-associated bone loss.

Acknowledgments We thank Dong-Su Jang, MFA (Medical Illustrator, Medical Research Support Section, Yonsei University College of Medicine, Seoul, Korea) for his help with the illustrations.

Compliance with Ethical Standards

Conflict of interest Keenan Brown is a stockholder of Mindways Software, Inc. Alan Brett and Keenan Brown are employees of Mindways Software, Inc. These affiliations do not affect the study results. Su Jin Lee, Kyoung Min Kim, J. Keenan Brown, Alan Brett, Yun Ho Roh, Dae Ryong Kang, Byeong Woo Park, and Yumie Rhee declare that they have no conflict of interest.

Human and Animal Rights and Informed Consent This is a retrospectively collected and analyzed study without any identifiable personal information which was approved by Institutional Review Board of Yonsei University Health System (IRB, No.4-2013-0685).

References

- Howell A, Cuzick J, Baum M, Buzdar A, Dowsett M, Forbes JF, Hochtin-Boes G, Houghton J, Locker GY, Tobias JS, Group AT (2005) Results of the ATAC (Arimidex, Tamoxifen, Alone or in Combination) trial after completion of 5 years' adjuvant treatment for breast cancer. *Lancet* 365:60–62
- Schairer C, Lubin J, Troisi R, Sturgeon S, Brinton L, Hoover R (2000) Menopausal estrogen and estrogen-progestin replacement therapy and breast cancer risk. *JAMA* 283:485–491
- Vestergaard P, Rejnmark L, Mosekilde L (2008) Effect of tamoxifen and aromatase inhibitors on the risk of fractures in women with breast cancer. *Calcif Tissue Int* 82:334–340
- Hille U, Soergel P, Langer F, Schippert C, Makowski L, Hillemanns P (2012) Aromatase inhibitors as solely treatment in postmenopausal breast cancer patients. *Breast J* 18:145–150
- Smith IE, Dowsett M (2003) Aromatase inhibitors in breast cancer. *N Engl J Med* 348:2431–2442
- Coomes RC, Kilburn LS, Snowdon CF, Paridaens R, Coleman RE, Jones SE, Jassem J, Van de Velde CJH, Delozier T, Alvarez I, Del Mastro L, Ortmann O, Diedrich K, Coates AS, Bajetta E, Holmberg SB, Dodwell D, Mickiewicz E, Andersen J, Lonning PE, Cocconi G, Forbes J, Castiglione M, Stuart N, Stewart A, Fallowfield LJ, Bertelli G, Hall E, Bogle RG, Carpentieri M, Colajori E, Subar M, Ireland E, Bliss JM, Study IE (2007) Survival and safety of exemestane versus tamoxifen after 2–3 years' tamoxifen treatment (Intergroup Exemestane Study): a randomised controlled trial. *Lancet* 369:559–570
- Eastell R, Hannon RA, Cuzick J, Dowsett M, Clack G, Adams JE (2006) Effect of an aromatase inhibitor on BMD and bone turnover markers: 2-year results of the anastrozole, tamoxifen, alone or in combination (ATAC) trial (18233230). *J Bone Miner Res* 21:1215–1223
- Servitja S, Nogues X, Prieto-Alhambra D, Martinez-Garcia M, Garrigos L, Pena MJ, de Ramon M, Diez-Perez A, Albanell J, Tusquets I (2012) Bone health in a prospective cohort of postmenopausal women receiving aromatase inhibitors for early breast cancer. *Breast* 21:95–101
- Chen Z, Maricic M, Bassford TL, Pettinger M, Ritenbaugh C, Lopez AM, Barad DH, Gass M, Leboff MS (2005) Fracture risk among breast cancer survivors: results from the Women's Health Initiative Observational Study. *Arch Intern Med* 165:552–558
- Body JJ (2011) Increased fracture rate in women with breast cancer: a review of the hidden risk. *BMC Cancer* 11:384
- Edwards BJ, Raisch DW, Shankaran V, McKoy JM, Gradishar W, Bunta AD, Samaras AT, Boyle SN, Bennett CL, West DP, Guise TA (2011) Cancer therapy associated bone loss: implications for hip fractures in mid-life women with breast cancer. *Clin Cancer Res* 17:560–568
- Yonden Z, Aydin M, Alcin E, Kelestemur MH, Kutlu S, Yilmaz B (2009) Effects of letrozole on bone biomarkers and femur fracture in female rats. *J Physiol Biochem* 65:267–275
- Hadji P, Body JJ, Aapro MS, Brufsky A, Coleman RE, Guise T, Lipton A, Tubiana Hulin M (2008) Practical guidance for the management of aromatase inhibitor-associated bone loss. *Ann Oncol* 19:1407–1416
- Nicks KM, Amin S, Melton LJ 3rd, Atkinson EJ, McCready LK, Riggs BL, Engelke K, Khosla S (2013) Three-dimensional structural analysis of the proximal femur in an age-stratified sample of women. *Bone* 55:179–188
- Ahmed LA, Center JR, Bjornerem A, Bluic D, Joakimsen RM, Jorgensen L, Meyer HE, Nguyen ND, Nguyen TV, Omsland TK, Stormer J, Tell GS, van Geel TA, Eisman JA, Emaus N (2013) Progressively increasing fracture risk with advancing age after initial incident fragility fracture: the Tromso study. *J Bone Miner Res* 28:2214–2221
- Tsa CH, Muo CH, Tzeng HE, Tang CH, Hsu HC, Sung FC (2013) Fracture in asian women with breast cancer occurs at younger age. *PLoS One* 8:e75109

17. Melton LJ 3rd, Hartmann LC, Achenbach SJ, Atkinson EJ, Thorneau TM, Khosla S (2012) Fracture risk in women with breast cancer: a population-based study. *J Bone Miner Res* 27:1196–1205
18. Cibula D, Skrenkova J, Hill M, Stepan JJ (2012) Low-dose estrogen combined oral contraceptives may negatively influence physiological bone mineral density acquisition during adolescence. *Eur J Endocrinol* 166:1003–1011
19. Neuner JM, Yen TW, Sparapani RA, Laud PW, Nattinger AB (2011) Fracture risk and adjuvant hormonal therapy among a population-based cohort of older female breast cancer patients. *Osteoporos Int* 22:2847–2855
20. Goss PE, Hershman DL, Cheung AM, Ingle JN, Khosla S, Stearns V, Chachal H, Rowland K, Muss HB, Linden HM, Scher J, Pritchard KI, Elliott CR, Badovinac-Crnjevic T, St Louis J, Chapman JA, Shepherd LE (2014) Effects of adjuvant exemestane versus anastrozole on bone mineral density for women with early breast cancer (MA.27B): a companion analysis of a randomised controlled trial. *Lancet Oncol* 15:474–482
21. Im GI, Lim MJ (2011) Proximal hip geometry and hip fracture risk assessment in a Korean population. *Osteoporos Int* 22:803–807
22. Ito M, Wakao N, Hida T, Matsui Y, Abe Y, Aoyagi K, Uetani M, Harada A (2010) Analysis of hip geometry by clinical CT for the assessment of hip fracture risk in elderly Japanese women. *Bone* 46:453–457
23. Adams JE (2009) Quantitative computed tomography. *Eur J Radiol* 71:415–424
24. Prevrhal S, Shepherd JA, Faulkner KG, Gaither KW, Black DM, Lang TF (2008) Comparison of DXA hip structural analysis with volumetric QCT. *J Clin Densitom* 11:232–236
25. Damilakis J, Maris TG, Karantanas AH (2007) An update on the assessment of osteoporosis using radiologic techniques. *Eur Radiol* 17:1591–1602
26. Khoo BC, Brown K, Zhu K, Price RI, Prince RL (2014) Effects of the assessment of 4 determinants of structural geometry on QCT- and DXA-derived hip structural analysis measurements in elderly women. *J Clin Densitom* 17:38–46
27. Cann CE, Adams JE, Brown JK, Brett AD (2014) CTXA hip-an extension of classical DXA measurements using quantitative CT. *PLoS One* 9:e91904
28. Williams N (2008) Effect of anastrozole and tamoxifen as adjuvant treatment for early-stage breast cancer: 100-month analysis of the ATAC trial. *Lancet Oncol* 9:45–53
29. Khosla S, Oursler MJ, Monroe DG (2012) Estrogen and the skeleton. *Trends Endocrinol Metab* 23:576–581
30. Almeida M, Iyer S, Martin-Millan M, Bartell SM, Han L, Ambrogini E, Onal M, Xiong J, Weinstein RS, Jilka RL, O'Brien CA, Manolagas SC (2013) Estrogen receptor- α signaling in osteoblast progenitors stimulates cortical bone accrual. *J Clin Invest* 123:394–404
31. Gregory JS, Aspden RM (2008) Femoral geometry as a risk factor for osteoporotic hip fracture in men and women. *Med Eng Phys* 30:1275–1286
32. Hadji P (2009) Aromatase inhibitor-associated bone loss in breast cancer patients is distinct from postmenopausal osteoporosis. *Crit Rev Oncol Hematol* 69:73–82
33. Bousson V, Le Bras A, Roqueplan F, Kang Y, Mitton D, Kolta S, Bergot C, Skalli W, Vicaud E, Kalender W, Engelke K, Laredo JD (2006) Volumetric quantitative computed tomography of the proximal femur: relationships linking geometric and densitometric variables to bone strength: role for compact bone. *Osteoporos Int* 17:855–864
34. Power J, Loveridge N, Lyon A, Rushton N, Parker M, Reeve J (2003) Bone remodeling at the endocortical surface of the human femoral neck: a mechanism for regional cortical thinning in cases of hip fracture. *J Bone Miner Res* 18:1775–1780
35. Poole KE, Mayhew PM, Rose CM, Brown JK, Bearcroft PJ, Loveridge N, Reeve J (2010) Changing structure of the femoral neck across the adult female lifespan. *J Bone Miner Res* 25:482–491
36. Johannesdottir F, Aspelund T, Reeve J, Poole KE, Sigurdsson S, Harris TB, Gudnason VG, Sigurdsson G (2013) Similarities and differences between sexes in regional loss of cortical and trabecular bone in the mid-femoral neck: the AGES-Reykjavik longitudinal study. *J Bone Miner Res* 28:2165–2176
37. Hangartner TN (2007) Thresholding technique for accurate analysis of density and geometry in QCT, pQCT and microCT images. *J Musculoskelet Neuronal Interact* 7:9–16
38. Hangartner TN, Short DF (2007) Accurate quantification of width and density of bone structures by computed tomography. *Med Phys* 34:3777–3784
39. Oken MM, Creech RH, Tormey DC, Horton J, Davis TE, McFadden ET, Carbone PP (1982) Toxicity and response criteria of the Eastern Cooperative Oncology Group. *Am J Clin Oncol* 5:649–655
40. Davis KA, Burghardt AJ, Link TM, Majumdar S (2007) The effects of geometric and threshold definitions on cortical bone metrics assessed by in vivo high-resolution peripheral quantitative computed tomography. *Calcif Tissue Int* 81:364–371
41. Cheung AM, Tile L, Cardew S, Pruthi S, Robbins J, Tomlinson G, Kapral MK, Khosla S, Majumdar S, Erlandson M, Scher J, Hu H, Demaras A, Lickley L, Bordeleau L, Elser C, Ingle J, Richardson H, Goss PE (2012) Bone density and structure in healthy postmenopausal women treated with exemestane for the primary prevention of breast cancer: a nested substudy of the MAP.3 randomised controlled trial. *Lancet Oncol* 13:275–284
42. Szabo KA, Webber CE, Adachi JD, Tozer R, Gordon C, Papaioannou A (2011) Cortical and trabecular bone at the radius and tibia in postmenopausal breast cancer patients: a peripheral quantitative computed tomography (pQCT) study. *Bone* 48:218–224
43. Bousson VD, Adams J, Engelke K, Aout M, Cohen-Solal M, Bergot C, Haguenaer D, Goldberg D, Champion K, Aksouh R, Vicaud E, Laredo JD (2011) In vivo discrimination of hip fracture with quantitative computed tomography: results from the prospective European Femur Fracture Study (EFFECT). *J Bone Miner Res* 26:881–893